ARCHIVIO ISTITUZIONALE
DELLA RICERCA

Alma Mater Studiorum Università di Bologna
Archivio istituzionale della ricerca

Field measurements on a large natural sand boil along the river Po, Italy

This is the final peer-reviewed author’s accepted manuscript (postprint) of the following publication:

Published Version:
Michela Marchi, M.F.G.M. (2021). Field measurements on a large natural sand boil along the river Po, Italy. QUARTERLY JOURNAL OF ENGINEERING GEOLOGY AND HYDROGEOLOGY, 54(4), 1-10 [10.1144/qjegh2020-097].

Availability:
This version is available at: https://hdl.handle.net/11585/818346 since: 2021-04-08

Published:
DOI: http://doi.org/10.1144/qjegh2020-097

Terms of use:

Some rights reserved. The terms and conditions for the reuse of this version of the manuscript are specified in the publishing policy. For all terms of use and more information see the publisher's website.

This item was downloaded from IRIS Università di Bologna (https://cris.unibo.it/).
When citing, please refer to the published version.

(Article begins on next page)

19 October 2024

Downloaded from http://qjegh.lyellcollection.org/ by guest on December 12, 2020

Accepted Manuscript

Quarterly Journal of Engineering Geology and Hydrogeology

Field measurements on a large natural sand boil along the river Po (Italy)

Michela Marchi, María Fernanda García Martínez, Guido Gottardi & Laura Tonni

DOI: https://doi.org/10.1144/qjegh2020-097

To access the most recent version of this article, please click the DOI URL in the line above.

Received 16 May 2020
Revised 25 November 2020
Accepted 8 December 2020

© 2020 The Author(s). Published by The Geological Society of London. All rights reserved. For permissions: http://www.geolsoc.org.uk/permissions. Publishing disclaimer: www.geolsoc.org.uk/pub_ethics

When citing this article please include the DOI provided above.

Manuscript version: Accepted Manuscript
This is a PDF of an unedited manuscript that has been accepted for publication. The manuscript will undergo copyediting, typesetting and correction before it is published in its final form. Please note that during the production process errors may be discovered which could affect the content, and all legal disclaimers that apply to the journal pertain.

Although reasonable efforts have been made to obtain all necessary permissions from third parties to include their copyrighted content within this article, their full citation and copyright line may not be present in this Accepted Manuscript version. Before using any content from this article, please refer to the Version of Record once published for full citation and copyright details, as permissions may be required.

Downloaded from http://qjegh.lyellcollection.org/ by guest on December 12, 2020

Field measurements on a large natural sand boil along the river Po (Italy)

Michela Marchi, María Fernanda García Martínez, Guido Gottardi, and Laura Tonni

Author 1 - Corresponding author

Michela Marchi, Assistant Professor

Department of Civil, Chemical, Environmental and Materials Engineering (DICAM), University of Bologna

Viale Risorgimento 2, 40136 Bologna (Italy)

Ph. +39 051 2093526

Mob. +39 347 1599613

ORCID number 0000-0001-6944-8856

e-mail: michela.marchi@unibo.it

Author 2

María Fernanda García Martínez, Research Fellow

Interdepartmental Centre for Industrial Research in Building and Construction (CIRI), University of Bologna, Bologna, Italy

ORCID number 0000-0003-3965-5023

Author 3

Guido Gottardi, Professor

Department of Civil, Chemical, Environmental and Materials Engineering (DICAM), University of Bologna, Bologna, Italy

ORCID number 0000-0003-4944-8212

Author 4

Laura Tonni, Associate Professor

Department of Civil, Chemical, Environmental and Materials Engineering (DICAM), University of Bologna, Bologna, Italy

ORCID number 0000-0002-9391-6661

ACCEPTED MANUSCRIPT

Downloaded from http://qjegh.lyellcollection.org/ by guest on December 12, 2020

Abstract

Sand boils are the surface manifestation of an erosion process, known as backward erosion piping, which may take place beneath river embankments during high-water events. The risk of embankment failure greatly increases in locations affected by sand boils. Numerous studies have been carried out, mainly at the laboratory scale, providing significant advancements in this field. Nonetheless, there is still a gap between research and practice that needs to be filled.

This study presents a set of field measurements carried out on a large sand boil reactivated near the toe of an embankment along the river Po (Italy). Hydraulic heads, velocity and discharge, concentration and pipe geometry were measured as a function of the water level in the river during the November 2018 flood. The collected data are compared to predictions of a theoretical model which provides the head loss in the vertical pipe. Furthermore, the local exit gradients, as deduced from measurements, are discussed, together with the operational critical gradients adopted in current design practice.

The collected data provide important input parameters for the calibration of analytical and numerical models, typically implemented to investigate the sand boil evolution and then to assess the backward erosion piping risk at real scale.

ACCEPTED MANUSCRIPT

Keywords

river embankment, sand boil, backward erosion piping, field measurement, water flow

Downloaded from http://qjegh.lyellcollection.org/ by guest on December 12, 2020

The phenomenon of sand boils near the toe of river embankments during high-water events is the manifestation of an internal erosion process, which may take place in the sandy aquifer underlying a water retaining structure (Fig. 1). This process, known as *backward erosion piping*, is basically caused by underseepage. A predisposing factor for backward erosion piping is undoubtedly represented by the local stratigraphic arrangement. The process can typically develop where the foundation soil of the river embankment is made of an impervious/semi-impervious layer ("blanket") confining a lower sandy aquifer (Fig. 1a). A free unfiltered exit in the blanket, as a weak spot, a ditch or a crack can capture the water flow with a consequent local increase of the seepage pressures and possible sand fluidisation. When the difference between the levels of the river and the water table landside reaches a critical value, the local hydraulic gradient at the open exit increases and the upward seepage pressures on the sand grains causes the erosion initiation. It looks like the sand is boiling, hence the expression "sand boil" (Fig. 2b).

The progression of the erosion process beneath the embankment can give rise to shallow pipes at the interface between the sandy aquifer and the blanket. The eroded soil grains are transported to the ground surface and deposited around the fluidised zone, creating a cone similar to a volcano crater (Fig. 2). The progression and widening of the horizontal pipes beneath the embankment may eventually result in a collapse of the water retaining structure, with catastrophic consequences. The occurrence of backward erosion piping is recognized to be one of the major causes of severe damage of river embankments. As such, the phenomenon represents a primary concern in the assessment of flood risk worldwide (e.g. Cao 1994; Richards and Reddy 2007; Robbins and Sharp 2016). Over the last decades, high-water events have become increasingly frequent, intense and persistent, both in Italy and in other countries in Europe, as a possible effect of climate change. This has produced, in turn, an increase of the risk of riverbank failure, including mechanisms triggered by piping.

ACCEPTED MANUSCRIPT

Downloaded from http://qjegh.lyellcollection.org/ by guest on December 12, 2020

Furthermore, the progressive rise in size of such flood embankments, aimed at preventing overtopping phenomena, results in higher hydraulic gradients near the riverbank toe, with an increase of piping risk.

At present, the actions typically taken by the flood management authorities during extreme events are limited at keeping under control the sand volcanos during reactivation. The most common emergency measure consists in promptly ringing sand boils with sand sacks (Fig. 2a and c), while permanent mitigation interventions, such as impermeable diaphragms and berms, are adopted only in a limited number of sites affected by more severe sand boils.

The ongoing research aims at introducing novel mitigation measures and effective design tools (Förster *et al.* 2019). However, the state of the art, developed in the last decades, mostly relies on small scale physical tests (e.g. Van Beek *et al.* 2011; Fleshman and Rice 2014; Chen *et al.* 2015; Vandenboer *et al.* 2018), lacking of a sound validation in natural environment.

This paper describes a set of field measurements carried out on a large diameter natural sand boil located near the toe of a major river embankment of the river Po (northern Italy), which is prone to recurrent reactivations during high-water events. Data were collected during the autumn 2018 high-water event, when the sand boil had reached an equilibrium phase after the reduction of the excess hydraulic head obtained by placing sand sacks around the exit hole.

The availability of a related crucial piece of information, such as hydraulic heads, water flow, velocities, concentration and pipe geometry, provides undoubtedly the opportunity to gain a better insight into the hydraulics of sand boils. More importantly, these measurements turn out to be the input parameters required in a number of predictive models, both analytical (e.g. Bezuijen *et al.*, 2019) and numerical (e.g. Vandenboer *et al.* 2014; Navin and Shewbridge 2017; García Martinez *et al.* 2018), recently proposed in the literature to assess the risk of backward erosion piping (either in terms of initiation/reactivation or progression). Various Finite Element (FE) numerical studies have indeed recognized the key role of size and

ACCEPTED MANUSCRIPT

Downloaded from http://qjegh.lyellcollection.org/ by guest on December 12, 2020

permeability of a local discontinuity through the blanket in the computation of pressures and gradients landside, as extensively discussed in García Martínez *et al.* (in press). Other theoretical models, such as those devised by Robbins *et al.* (2019) or Bezuijen *et al.* (2019) to identify critical conditions for backward erosion piping progression, predict the possible head drop in a vertical pipe as a function of discharge and outflow velocity. However, although all these methods have proved to be very effective in modelling concentrated flow, the lack of reliable field data does not enable to extensively adopt such advanced predictive tools. Hence, the field measurements discussed in this paper turn out to be very useful to help reducing the parameter uncertainties of a reliable piping model.

ACCEPTED MANUSCRIPT

From research to practice

The main phases of the process, which have been identified through small-scale physical models (Van Beek *et al.* 2013), can be summarized as follows:

1. Single grain transport with development of flow path (micro-scale holes).
2. Boiling phase, with the fluidisation of soil in the vertical exit pipe, although without deposition of sand around the center of the sand boil.
3. Regressive phase, characterized by sand transport and deposition near the exit point, with formation of small pipes within the sandy body. During this phase, due the changes in local hydraulic conditions caused by pipe growth, the piping process may reach equilibrium even though the hydraulic load has not changed. For this reason, regressive phase is also known as equilibrium phase. However, in predominantly plane (i.e. without the blanket at the toe of the embankment, landside) and ditch-type experiments, equilibrium is not observed, thus implying that the critical head for progression is exceeded since the beginning of pipe formation.
4. Progressive backward erosion phase, with pipes development towards the river

Downloaded from http://qjegh.lyellcollection.org/ by guest on December 12, 2020

(horizontal pipe at the contact with the aquifer), at times requiring further increase of head drop, eventually leading to the collapse of the embankment.

With respect to the above phases, data presented in this study refer, in particular, to the equilibrium phase of a sand boil, with the concentrated flow causing the sand to fluidise in a pre-existing spot.

Following the interpretation described in Robbins *et al.* (2019), the measurements presented herein provides the head loss in the sand boil (vertical pipe) only, the whole head loss in backward erosion piping process being also due to head loss in the horizontal pipe and to seepage riverside.

The large amount of laboratory experimental tests (De Wit *et al.* 1981; Müller-Kirchenbauer *et al.* 1993; Schmertmann 2000; Van Beek 2015 among others), most of them based on 2D configurations, have led to the development of analytical methods for the prediction of piping progression (e.g. Sellmeijer and Koenders 1991). However, apart from scale effects mainly due to aquifer depth, critical gradients predicted in small scale experiments do not typically consider 3D flow (as emphasized by Vandenboer 2019 or Van Beek *et al.* 2013), nor heterogeneity of natural soil deposits (Kanning 2012). Accordingly, extending the results of laboratory tests to natural field conditions is not always straightforward and effective.

Investigations on natural sand boils are undoubtedly rare. Difficulties in collecting field measurements during piping are primarily due to the occasional occurrence of sand boil activation or reactivation, but also to the priority taken by the emergency operations over any other collateral activity, especially in case of large sand boils. This may explain why the data collected over the last decades in the Mississippi sand boils (Robbins *et al.* 2019; USACE 1956) still remain the most significant and exhaustive information currently available on natural sand boils. These data have been indeed used as reference database to define empirically-derived criteria for piping reactivation (USACE 1956; 2000).

ACCEPTED MANUSCRIPT

Downloaded from http://qjegh.lyellcollection.org/ by guest on December 12, 2020

The investigation site

In northern Italy, sand boils are often observed, especially along the major Italian watercourse Po and its tributaries, which cross a densely populated and highly developed territory. Indeed, the typical stratigraphic arrangement of the river Po embankments may create favourable conditions for the occurrence of backward erosion piping. In this area, during the 20th century the embankments have been reshaped and their size has been increased, in an attempt to contain the progressive water level rise. While preventing overtopping, at the same time modifications in geometry have resulted in higher hydraulic heads and thus in an increase of vulnerability towards piping phenomena.

A total of 130 sand boils have been catalogued in recent years along the river Po (Aielli *et al.* 2019). Among them, about 80 are present along the main course of the river and are subjected to reactivations during high-water events. By contrast, the sand boils located in the Delta area reactivate also at relatively moderate water levels . This is typical of lowland riverine environments, where the elevation of the river bed is generally higher than the ground level landside, resulting in high values of the hydraulic excess head also in the dry season.

During the severe high-water event occurred in 2000, a large part of these sand boils reactivated simultaneously. Furthermore, it is worth mentioning that sand boils observed along the river Po have a remarkable size, typically larger than many other piping evidences observed in other European basins. In some cases, sand volcanos may have an external diameter higher than 3 m. This might imply an ongoing significant erosion process beneath the river embankment, with potentially severe effects on the structure stability.

The investigated section is located near Guarda Ferrarese, in the lower catchment of the river Po. Figure 3 shows its stratigraphic arrangement, as obtained from CPTU tests (Gottardi *et al.* 2015). It is worth observing that the presence of a sandy aquifer (unit A), 9-12 m thick,

ACCEPTED MANUSCRIPT

Downloaded from http://qjegh.lyellcollection.org/ by guest on December 12, 2020

confined by a 3 m thick impermeable top layer (units B and C), makes the section prone to backward erosion piping phenomena. Furthermore, the potential susceptibility to backward erosion piping was increased by the excavation of a ditch parallel to the road embankment (Fig. 3). In this area, indeed, a “historical” sand boil has suffered recurrent reactivations during past high-water events (García Martínez *et al.* 2020). The most recent reactivations date back to 2014, 2018 and 2020. During the first event, the violence of the reactivation was due to the high-water level in the river and an external sand volcano, 2.5 m wide, formed around the exit hole. In that occasion, sand sacks had to be placed not only around the sand boil, but also at its sides, where two sand boils break out beyond the limits of these sacks (Fig. 2c). In the 2018 reactivation, a 1 m diameter volcano developed around the sand boil exit, in spite of a moderate flood intensity. Finally, in 2020, reactivation was again clearly detected. Heavy flow through the vertical pipe with transport of finer sand grains was observed.

ACCEPTED MANUSCRIPT

Field measurements on the sand boil in November 2018

The reactivation of November 2018 provided the conditions to carry out a field investigation on the sand boil. The geometry of the exit hole and the flow conditions inside the vertical pipe were mainly taken into consideration. The following parameters, in particular, were measured: hydraulic heads along the vertical pipe (i.e. head loss), velocities, discharge (flow), and geometry.

Samples of soil were collected from the fluidised sand in the vertical pipe and from the external volcano (Fig. 4a), in order to obtain their grain size distribution. The first sample of fluidised sand, collected in the vertical pipe using a disposal bailer sampler, was also used for measuring concentration of the sand-water mixture. Shortly after the reactivation, on November 1st, the sand boil discharged considerable material. Then, sand sacks were placed

Downloaded from http://qjegh.lyellcollection.org/ by guest on December 12, 2020

around the active sand boil to ring it, thus causing an increase of the water head in the ditch. Measurement of the whole set of parameters could be carried out only on November 9th, whilst in the other dates (November 7th, 11th and 20th) only depth of the vertical pipe and head loss were monitored. The water level variation in the river during this time lapse was recorded by two hydrographic stations close to the investigated section (Fig. 4b). All the measurements were carried out after the ringing of the sand boil, when the sand boil was in an equilibrium phase: sand was fluidised inside the pre-existing vertical pipe and transported through the spot but not considerably ejected from the exit hole. Only finer particles were discharged to the ground surface during the monitoring dates November 7th, 9th and 11th, while no solid transport was visible on the last day of readings (20th November).

Vertical pipe geometry: external volcano, horizontal section and depth

The geometry of the vertical pipe was investigated using a rod and a standard wooden ruler. As shown in the schematic section of Figure 4a, a volcano of sand ejected from the pipe during the initial phase of reactivation could be clearly observed around the exit hole, at the ground surface (base of the ditch). The dimensions of the volcano crater were measured on November 9th. It had a diameter of about 1 m at the top of the rim and was approximately 15 cm high. On the same day, the vertical pipe was found to have a funnel shape, its width (*D*) showing a tendency to increase from about 20 cm at its bottom to approximately 35 cm near the exit. The geometry of the external volcano and the horizontal sections of the vertical pipe did not change significantly during the monitoring period. On the contrary, the vertical pipe length was sensitive to the oscillations of the river water level, varying from a maximum of 1.54 m to a minimum of 0.73 m the last day of readings (see data reported in table 1). It is known indeed that an increase of the river water level results in a higher water pressure at the base of the vertical pipe, causing in turn further fluidization of the sand and deepening of the

ACCEPTED MANUSCRIPT

Downloaded from http://qjegh.lyellcollection.org/ by guest on December 12, 2020

pipe itself. On the other hand, during the last day of readings, the vertical pipe was half filled due to re-deposition of the previously eroded sand.

Water head in the vertical pipe

Water heads along the vertical pipe were measured by means of a transparent, 1 cm diameter PE tube connected to a rod. A filter was placed at the base of the tube in order to prevent inflow of particles (Fig. 5). By lowering the system into the sand boil, the water head at different depths could be measured as water rise into the transparent tube. At present, the installation of permanent piezometers inside vertical pipes or in proximity of the sand boils is not permitted by the Interregional Agency for the River Po (AIPo). The results of the measurements, plotted in Figure 6 and summarized in Table 1, need to be analysed in conjunction with both the river water levels (z_w), shown in the hydrograph of Figure 4b, and, in particular, with the relevant overall hydraulic head drop between the river and the ditch ($\Delta H_{river\text{-}ditch}$). The hydrograph is indeed characterized by a sequence of rising and recession limbs during the monitoring period (November 7th - 20th), with two short plateaux. An overall increment of the river water level equal to 1.27 m was observed from November 7th to November 11th, (days 1 and 3), followed by a drop of 3.99 m between day 3 and day 4.

According to the measurements reported in Figure 6, the variations of the head loss between the river and the ditch ($\Delta H_{river\text{-}ditch}$) result in a variation of the pressure head at the pipe base ($h_{pipe\ base}$ in Table 1) and in a deepening of the vertical pipe (increase of L). At the same time, the hydraulic head drop between the base of the vertical pipe and the ditch (ΔH) is found to be not appreciable within the accuracy of the adopted measure technique in the rising limbs of the hydrograph.

The measurements of the hydraulic head drop between the base of the vertical pipe and the ditch (ΔH), coupled with the information on the pipe lengths (L), can be first used to determine the average gradient in the vertical pipe (i), which was found to vary between 0.46

ACCEPTED MANUSCRIPT

Downloaded from http://qjegh.lyellcollection.org/ by guest on December 12, 2020

and 0.53 during the monitoring period (Table 1). It is worth emphasizing that these values do not correspond to a phase involving sand ejection outside the pipe. Nonetheless, these gradients are high enough to bring sand grains into the water suspension inside the vertical pipe, thus resulting in an increase of its depth, along with a consequent higher concentration of the sand-water mixture inside the hole.

On the other hand, the absence of significant variations in head drop across the vertical pipe (ΔH) suggests that during the monitoring period, to be interpreted as a sequence of equilibrium stages characterized by different water heads imposed by the river, the variation of hydraulic head loss governing underseepage ($\Delta H_{river\text{-}ditch}$) is very likely to have been absorbed for fluidization of the sand bed in the vertical pipe (ΔL), since only minor changes in the average hydraulic gradient into the vertical pipe are observed (i in Table 1).

Flow velocity and discharge

Direct measurements of flow velocity have been carried out using two different procedures, based on the use of a portable digital flow meter and dye injections. However, both methods provided only a rough estimate of the actual flow velocity. The portable digital flow meter (Fig. 7) had been tested before in another large sand boil at the onset of reactivation, providing a flow velocity in the range 0.4 and 0.7 m/s. In the case described in this paper, the rate was lower than the instrument sensitivity (0.1 m/s), hence the instrument could only provide an upper boundary of the real rate. Such an observation was confirmed by the result of the dye injections, carried out through a needle connected to a syringe (Robbins *et al.* 2019). The syringe was filled with a diluted food industry dye and lowered into the vertical pipe using a rod. From the bottom of the vertical pipe the dye was then injected. The time required for the coloured fluid to resurface was estimated to be about 12 s. Unfortunately, this measurement is affected by some uncertainty, since the exit instant of the dye from the exit hole was not clearly identifiable because of the cloudy and dark colour of the water.

ACCEPTED MANUSCRIPT

Downloaded from http://qjegh.lyellcollection.org/ by guest on December 12, 2020

Considering that the length of the vertical pipe was approximately 1.5 m, the estimated flow velocity is likely to be about 0.1 m/s.

Discharge was determined by measuring the volume of water overflowing from both side of the ditch, at regular time intervals. Graduated buckets were used to measure the water volume. The average value of discharge, as deduced from 4 independent readings, was estimated to be close to 2 l/s, also considering a probable loss of 10%. This value of discharge can be used to obtain an indirect estimation of the velocity of the flow through the vertical pipe. In fact, assuming the water head as constant during the measurement, for a 0.2 m diameter pipe, the velocity of the water flow turns out to be about 0.06 m/s.

Sample collection and laboratory tests

Concentration

Concentration is a significant parameter that affects transport of solid particles in solid-liquid suspensions (Baldock *et al.* 2004). It is useful for the calculation of critical transport velocity and thus for the identification of the reactivation conditions of sand boils. An example is provided by Vandenboer (2019) and Robbins *et al.* (2019), who investigated the relationship between concentration of sand-water mixtures and head drop causing sand ejection. This parameter has been also found to be crucial for the proper characterization of the vertical pipe volume in finite element analysis of sand boil reactivations, as shown in the study by García Martínez *et al.* (in press). In current practice, this measure is typically extrapolated from discharge and velocity data, instead of being directly determined.

The fluidised sand into the vertical pipe was sampled using a disposable PVC bailer (length 91 cm, diameter 3,81 cm) (Fig. 8A and B). Disposable bailers are devices commonly used in ground water monitoring wells to retrieve water samples. The sampler used in this campaign consisted of a hollow tube with a check valve at its bottom and a handle at the top, connected

ACCEPTED MANUSCRIPT

Downloaded from http://qjegh.lyellcollection.org/ by guest on December 12, 2020

to a rod which was lowered into the vertical pipe in order to retrieve the water sample. Hydrostatic pressure of the fluid pushed up the check valve, thus enabling the water to flow into the tube. When the disposable bailer had filled to its submerged level, the valve closed, preventing water outflow. The sample was put into a 1l jar (Fig. 8C) and sent to the laboratory for the determination of solid volumetric concentration C_v and the grain size characteristics.

The concentration is defined as the ratio of the amount of solids to the total mixture, given by:

$$C_v = {}^{V_{solid}}\big/_{(V_{solid} + V_{water})} \qquad (1)$$

where V_{solid} is the volume of the solid particles and V_{water} is the volume of pore water. For fully saturated soils, C_v can be written as $C_v = 1/(1+e) = 1\text{-}n$, being e the void ratio and n the porosity.

With respect to the collected sample, V_{solid} = 270.47 cm^3 (weight 723.22 g) and V_{water} = 585.47 cm^3 (weight 585.67 g), resulting in a concentration equal to C_v = 31.6 %. This value can be compared with an independent, indirect determination of C_v obtained

by using the equation described in Vandenboer (2019), which expresses the excess water head at the base of the vertical pipe at the verge of sand ejection (i.e. between boiling phase and grain ejection phase) as a function of concentration, water density (ρ_w), particle density (ρ_s) and depth of the vertical pipe (L):

$$\Delta H = C_v \cdot L \cdot \frac{\rho_s - \rho_w}{\rho_w} \qquad (2)$$

For ΔH = 0,77 m, L = 1,51 m and ρ_s = 2650 kg/m^3, concentration turns out to be 0,309, which is very close to the experimental determination.

Particle size distribution

Particle size distribution was determined on no. 3 disturbed sand samples collected from the

ACCEPTED MANUSCRIPT

Downloaded from http://qjegh.lyellcollection.org/ by guest on December 12, 2020

fluidised sand in the vertical pipe (bailer sampler) and from the external volcano, by hand. The resulting grain size distribution curves are plotted in Figure 9.

The comparison of the curves shows that the finer sand particles were ejected from the pipe (Sample 1) during the initial phases of the sand boil reactivation, typically characterized by transport of grains outside the pipe. Coarser particles remained instead suspended into the water inside the vertical pipe, hence the slightly coarser grain size of samples 2 and 3, both collected from the fluidised sand in the vertical pipe. Unfortunately, soil samples from the aquifer are not yet available for this specific river embankment cross section.

Application of an analytical model for the interpretation of hydraulic heads in the sand boil

This section provides an attempt to interpret the measurements described above in the light of a theoretical model (Robbins *et al.* 2019) devised to predict the amount of head loss across a sand boil. According to this approach, in steady state conditions the total head loss $H_T(z)$ is obtained by integrating the two contributions ($\partial H_L/\partial z$) and ($\partial H_D/\partial z$) over the entire sand boil length:

$$H_T(z) = \int_0^z \left(\frac{\partial H_L(z)}{\partial z} + \frac{\partial H_D(z)}{\partial z}\right)\partial z = \int_0^z \left[\left(\frac{32\mu v(z)}{\rho_w g D(z)^2}\right) + (G_s - 1)C_V(z)\right]\partial z \qquad (3)$$

where H_L and H_D are the head loss caused by fluid flow and by the drag force applied on suspended sediments, respectively. As shown by Equation 3, the model explicitly requires flow velocity ($v(z)$), concentration ($C_v(z)$), particle specific gravity (G_s) and the diameter of the hole throughout the entire sand boil profile ($D(z)$) as input parameters. Additionally, fluid density (ρ_w), dynamic fluid viscosity (μ) and gravity acceleration (g) must be specified. It is worth observing that v(z) in Equation 3 is in turn calculated as a function of the discharge (Q), while the C_v profile along the sand boil is determined according to the procedure described in Baldock *et al.* (2004).

ACCEPTED MANUSCRIPT

Downloaded from http://qjegh.lyellcollection.org/ by guest on December 12, 2020

In agreement with field observations, the vertical pipe diameter was assumed to vary linearly over the entire length (L = 1,51 m) of the vertical exit hole, namely from 0.35 m on top to 0.20 m at the base. The ejected sand was spread over a rather large area around the exit hole, hence the resulting sand volcano appeared to have a gentle slope (α), approximately equal to 15°.

As suggested by Robbins *et al.* (2019), the particle diameter d_{80} (≈ 0.35 mm from particle size distribution of Fig. 9) was used to estimate the C_v profile along the sand boil, also taking into account a maximum concentration equal to 0.6. With regard to the discharge, the value measured on November 9th (Q = 2 l/s) was used for prediction.

Table 2 summarizes the set of parameters adopted in the application of the model. Figure 10 shows the values predicted by the model and the local head loss measured on November 9th. The theoretical head profile appears to be in good agreement with field measurements, with a tendency to underestimate the excess head moving towards the base of the vertical pipe. As reported in the Figure, the error associated with predictions falls in the range 9.4 % ÷ 23.5 %. The order of magnitude of the measured and predicted values of excess heads in the investigated sand boil have the same order of magnitude of the data described by Robbins et al. (2019) for the IJzendoorn sand boil along the river Waal in the Netherlands.

Analysis of piping vulnerability through field observations: a comparison with existing databases

Field observations described in this paper could mainly contribute to models describing the transport of particles to the ground surface and head losses in the vertical spot. Furthermore, a comparison between observations on the investigated sand boil along the river Po and those on the Mississippi, widely documented in USACE 1956, could provide an interesting point of view on the reported case study.

ACCEPTED MANUSCRIPT

Downloaded from http://qjegh.lyellcollection.org/ by guest on December 12, 2020

The USACE (1956) database, which describes 16 instrumented river sections along the Mississippi, was used to develop the well-established analytical solution for assessing under-seepage, known as blanket theory. The same data were also used to derive the operational vertical exit gradient in the top stratum, equal to 0,5, currently used in the US for the design of hydraulic structures against piping. This empirically-derived criterion, coupled with the blanket theory, is basically the only method existing in literature for the assessment of initiation of backward erosion piping. The other existing approaches (Sellmeijer 1988, Sellmeijer and Koenders 1991, Sellmeijer et al. 2011, among others) are indeed focused on failure of the river embankment, when excessive growth of pipes beneath the embankment foundation occurs.

The vertical exit gradients in the top stratum specified in USACE (1956) correspond to the onset of new activation or reactivation of a sand boil. Their values were deduced by means of hydraulic heads near the toe of the river embankment, provided by piezometers installed in proximity of the sand boils, divided by the thickness of the top stratum. When comparing the above gradients with those reported in Table 1 for the river Po, it should be emphasized that the latter values arise from excess water heads measured during boiling at the base of the vertical pipe, divided by the throat length (L). In spite of such differences in measurement procedure, both of them represent average exit values of the vertical gradients in the top stratum, thus the comparison provided in Fig. 11 appears reasonable. Following a previous USACE (1956) data representation, also accounting for the intensity/severity of phenomenon, all the data fall in the same domain, corresponding to the sand boil occurrence. The Figure suggest that the gradients computed for the river Po are consistent with those reported in USACE (1956).

ACCEPTED MANUSCRIPT

Discussion of results and final remarks

Downloaded from http://qjegh.lyellcollection.org/ by guest on December 12, 2020

The most significant outcomes of this paper can be summarized as follows:

1) A valuable piece of information has been obtained for the investigated natural sand boil, in terms of vertical pipe diameter and depth, particle size of both fluidised and ejected sediments. These data, which are not routinely obtained in practice, are of crucial importance for the calibration of piping models.

2) A novel way of measuring concentration of suspended particles in the pipe during reactivation has been introduced and its effectiveness demonstrated by comparison with independent determinations of C_v from discharge and velocity data. Concentration is a relevant parameter for the analysis of the hydraulics of a sand boil and in the definition of reactivation criteria, but it had never been measured before in a natural sand boil.

3) Good agreement has been found between measured head loss in the vertical pipe and that deduced from the application of Robbins *et al.* (2019) model. When applied to the river Po case, the model provides trends of hydraulic gradients similar to the values predicted for the Dutch sand boil described in the same study (Robbins *et al.* 2019).

4) The observed evolution of excess water head into the vertical pipe suggests that during the monitoring period, which can be interpreted as a sequence of equilibrium stages characterized by different water heads imposed by the river, the variation of hydraulic load governing underseepage is very likely to have been partly absorbed by fluidisation of the sand bed in the vertical pipe and partly dissipated in the aquifer along the seepage length. Indeed, only minor changes in the average hydraulic gradient at the base of the vertical pipe were observed.

5) The vertical exit gradients computed for the river Po section have been compared with those observed in the river Mississippi and described in USACE (1956). In spite of the differences in the calculation procedure adopted for the two different datasets, as described in the text, the values turn out to be in good agreement.

ACCEPTED MANUSCRIPT

Downloaded from http://qjegh.lyellcollection.org/ by guest on December 12, 2020

The novel data herein discussed can represent a useful contribution to a better understanding of piping phenomena in natural environment and a valuable piece of information for the calibration of suitable models to be used in risk assessment procedures and for the design of relevant mitigation measures.

Acknowledgements

The authors would like to acknowledge all people at the Interregional Agency for the river Po (AIPO), who offered valuable and constant support and provided permissions to access to the investigated area.

List of notations

A	cross-sectional area of the vertical pipe
C_v	volumetric concentration
D	vertical pipe diameter
d_{80}	particle size diameter for which 80% of the particles are smaller
e	void ratio
g	gravitational acceleration
G_s	particle specific gravity
H_D	head loss due to particle drag
H_L	head loss due to fluid flow
H_T	total head loss through the sand boil
$h_{pipe\ base}$	pressure head at the base of the vertical pipe
i	average hydraulic gradient in the vertical pipe
L	vertical pipe length
n	porosity

ACCEPTED MANUSCRIPT

Downloaded from http://qjegh.lyellcollection.org/ by guest on December 12, 2020

Q	discharge out of the sand boil
r	vertical pipe radius
v	water flow velocity
V_{solid}	volume of solid particles
V_{water}	volume of pore water
z_w	river water levels
ΔH	head loss across the vertical pipe
$\Delta H_{river\text{-}ditch}$	head loss between the river and the ditch
α	angle of the interior sand cone slope with the horizontal
μ	dynamic viscosity of water
ρ_w	density of water
ρ_s	density of sand particles

References

Aielli, S., Pavan, S., Parodi, S., Rosso, A., Tanda, M.G., Marchi, M., Vezzoli, G., Pantano, A., Losa, D. and Sirtori, M. 2019. Collection and analysis of the reactivation data of the historical sand boils in the po river levees. *In:* Bonelli, S., Jommi, C. & Sterpi, D. (eds) *Internal Erosion in Earthdams, Dikes and Levees, Proceedings of EWG- IE 26th Annual Meeting 2018*. Springer, Switzerland, Lecture Notes in Civil Engineering, 327-335, https://doi.org/10.1007/978-3-319-99423-9_29

Baldock, T.E., Tomkins, M.R., Nielsen, P. and Hughes, M.G. 2004. Settling velocity of sediments at high concentrations. Coastal Engineering, **51**(1), 91-100, https://doi.org/10.1016/j.coastaleng.2003.12.004

ACCEPTED MANUSCRIPT

Downloaded from http://qjegh.lyellcollection.org/ by guest on December 12, 2020

Bezuijen, A., Vandenboer, K., Van Beek, V. and Robbins, B. 2019. Pressure drop in vertical pipes of sand boils. *In: Geotechnical Engineering foundation of the future, Proceedings of the XVII ECSMGE,* https://doi.org: 10.32075/17ECSMGE-2019-0154

Cao, D. 1994. Countermeasures for seepage erosion of Yangtze River main dikes. *Yangtze River*, **25**(1), 25-30.

Chen, J., S. Wang, Y. Liang, Y. Wang, and Y. Luo. 2015. Experimental investigation of the erosion mechanisms of piping. *Soil Mech. and Foundation Eng.*, **52**, 301-309.

De Wit, J.M., Sellmeijer, J.B. and Penning, A. 1981. Laboratory testing on piping. *In: Proc. 10th International Conference on Soil Mechanics and Foundation Engineering*, 517-520.

Fleshman, M.S. and Rice, J.D. 2014. Laboratory Modeling of the Mechanisms of Piping Erosion Initiation. *J. Geotech. Geoenviron. Eng.*, **140**, 04014017, https://doi.org/10.1061/(ASCE)GT.1943-5606.0001106

García Martínez, M.F., Tonni, L., Marchi, M., Tozzi, S. and Gottardi, G. A numerical tool for the prediction of sand boil reactivations near river embankments. Journal of Geotechnical and Geoenvironmental Engineering, in press, https://doi.org/10.1061/(ASCE)GT.1943-5606.0002380

García Martínez, M.F., Gottardi, G., Marchi, M. and Tonni, L. 2018. Modelling a sand boil reactivation in the middle-lower portion of the Po River banks. *In: Proc. 9th European Conf. on Numerical Methods in Geotech. Eng.* (*NUMGE*), 1219-1225.

García Martínez, M.F., Gottardi, G., Marchi, M. and Tonni, L. 2020. On the reactivation of sand boils near the Po River major embankments. *In:* Calvetti, F, Cotecchia F., Galli, A. and Jommi, C. (eds) *Geotechnical Research for Land Protection and Development, Proceedings of CNRIG 2019.* Springer, Switzerland, Lecture Notes in Civil Engineering, 328-337, https://doi.org/10.1007/978-3-030-21359-6_35

ACCEPTED MANUSCRIPT

Downloaded from http://qjegh.lyellcollection.org/ by guest on December 12, 2020

Gottardi, G., Marchi, M. and Tonni, L. 2015. Static stability of Po river banks on a wide area. *In: Geotechnical Engineering for Infrastructure and Development. Proc. of the XVI European Conference on Soil Mechanics and Geotechnical Engineering (ECSMGE 2015*), 1675-1680.

Kanning, W. 2012. *The weakest link – length effects for piping*. Phd thesis, Delft University of Technology, Delft, The Netherlands.

Müller-Kirchenbauer, H., Rankl, M. and Schlötzer C. 1993. Mechanism for regressive erosion beneath dams and barrages. In *Filters in Geotechnical and Hydraulic Engineering*, 369-376. Balkema, Rotterdam.

Navin, M.P. and Shewbridge, S.E. 2017. Example of 2D Finite Element analyses to inform backward Erosion Piping Evaluation of a Typical Levee Cross-Section. *In: Proc. Geo-Risk 2017, ASCE Geotechnical Special Publication* GSP 284, 32–45, https://doi.org/10.1061/9780784480717.004

Richards, K.S. and Reddy, K.R., 2007. Critical appraisal of piping phenomena in earth dams. Bulletin of Engineering Geology and the Environment **66** (4), 381-402, https://doi.org/10.1007/s10064-007-0095-0

Robbins, B.A., and Sharp, M.K. 2016. Incorporating uncertainty into backward erosion piping risk assessments. *In*: Lang, M., Klijn, F. and Samuels, P. (eds.) *Proc. 3rd European Conference on Flood Risk Management (FLOODrisk 2016)*, Article number 03007. E3S Web of Conferences, EDP Sciences, https://doi.org/ 10.1051/e3sconf/20160703007.

Robbins, B.A. and Griffiths, D. V. 2019. A new fragment for seepage beneath impervious structures. *Geotechnique*, **69**, 174–179, https://doi.org/10.1680/jgeot.17.P.209

Robbins, B.A., Stephens, I.J., Van Beek, V., Koelewijn, A.R. and Bezuijen, A. 2019. Field measurements of sand boil hydraulics. *Géotechnique*, **70** (2), 153-160.

ACCEPTED MANUSCRIPT

Downloaded from http://qjegh.lyellcollection.org/ by guest on December 12, 2020

Schmertmann, J.H. (2000). The non-filter factor of safety against piping through sands. *In: Judgment and innovation the heritage and future of the geotechnical engineering profession, ASCE Geotechnical Special Publication GSP111*, 65–132. Reston, USA.

Sellmeijer, J.B. and Koenders, M.A., 1991. A mathematical model for piping. *Applied Mathematical Modelling*, **15** (11-12), 646-651.

Sellmeijer, J.B. 1988. *On the mechanism of piping under impervious structures*. PhD Thesis, Technical University of Delft, Delft, The Netherlands.

Sellmeijer, H., de la Cruz, J.L., Van Beek, V. and Knoeff, H. 2011. Fine-tuning of the backward erosion piping model through small-scale, medium-scale and IJkdijk experiments. *European J. of Environmental and Civil Engineering*, **15**(8), 1139-1154.

USACE 2000. *Design and construction of levees*. EM 1110-2-1913. Washington, DC.

USACE 1956. *Investigation of underseepage and its control, lower Mississippi River levees* (TM-3-424). Vicksburg, MS, USA.

Van Beek, V., Knoeff, H. and Sellmeijer, H. 2011. Observations on the process of backward erosion piping in small-, medium- and full-scale experiments. *European Journal of Environmental and Civil Engineering*, **15**, 1115-1137, https://doi.org/10.1080/19648189.2011.9714844

Van Beek, V.M., Bezuijen, A. and Sellmeijer, H. 2013. Backward erosion piping. *In*: Bonelli, S. and Nicot, F. (eds) *Erosion in Geomechanics Applied to Dams and Levees*. Wiley, 193–269.

Van Beek, V. M. 2015. *Backward erosion piping: initiation and progression*. PhD Thesis, Technishe Universiteit Delft, Delft, the Netherlands.

Vandenboer, K., Van Beek, V and Bezuijen A. 2014. 3D finite element method (FEM) simulation of groundwater flow during backward erosion piping. *Front. Struct. Civ. Eng.*, **8**(2), 160–166.

ACCEPTED MANUSCRIPT

Downloaded from http://qjegh.lyellcollection.org/ by guest on December 12, 2020

Vandenboer, K., Van Beek, V. and Bezuijen, A. 2018. 3D character of backward erosion piping. *Géotechnique*, **68**, 86-90, https://doi.org/10.1680/jgeot.16.P.091

Vandenboer, K., 2019. *A Study on the Mechanisms of Backward Erosion Piping*. PhD Thesis, University of Gent (Belgium), ISBN 978-94-6355-208-0

ACCEPTED MANUSCRIPT

Downloaded from http://qjegh.lyellcollection.org/ by guest on December 12, 2020

Caption List

Fig. 1. Schematic drawing of backward erosion process, from (**a**) piping initiation to (**b**) failure of the river embankment.

Fig. 2. Photographs of sand boils along the river Po in Italy: (**a**) ringing of a large sand boil in Boretto (Reggio Emilia Province) reactivated in 2000. In the investigated sand boil (in Guarda Ferrarese): (**b**) sand boiling before ringing with sand sacks in 2018 (approx. diameter of the external sand volcano: 1 m) and (**c**) ringed sand boil after the 2014 flooding (approx. diameter of the external sand volcano: 2.5 m).

Fig. 3. Stratigraphic cross-section of the investigated section with CPTU log profiles (vertical scale magnified).

Fig. 4. (**a**) Scheme of the pipe geometry and sample positions; (**b**) Hydrograph of November 2018 flood.

Fig. 5. Details of the filter placed at the lower end of the PE tube used for the measurement of water heads.

Fig. 6. Water head distribution along the pipe, as measured in the four different days of investigation.

Fig. 7. Details of the portable digital flow meter used to measure flow velocity.

Fig. 8. Frame (**a**): Sketch of the sampling operations inside the pipe with detail of the bailer tip during filling. Frame (**b**): photo of the PVC disposable bailer sampler. Frame (**c**): 1 litre jar used for sampling.

Fig 9. Grain size distribution curves of the samples collected in the sand boil.

Fig 10. Comparison between excess head predicted by the Robbins *et al.* (2019) theoretical model and values measured on November 9th.

Fig 11. Comparison between the average hydraulic gradients in the fluidised sand in the vertical pipe measured in this study and the maximum upward gradients through the top

ACCEPTED MANUSCRIPT

Downloaded from http://qjegh.lyellcollection.org/ by guest on December 12, 2020

stratum observed in 1950 along the Mississippi river (data from USACE 1956), as measured by piezometers at various sites were sand boils were observed. Gradients are plotted as a function of the severity of boiling.

Table 1. *Field measurements and deduced hydraulic gradients in the fluidised vertical pipe at different river stages.*

Table 2. *Input parameters of the analytical model (Robbins et al. 2019) adopted for the interpretation of hydraulic loads in the sand boil*.

ACCEPTED MANUSCRIPT

Downloaded from http://qjegh.lyellcollection.org/ by guest on December 12, 2020

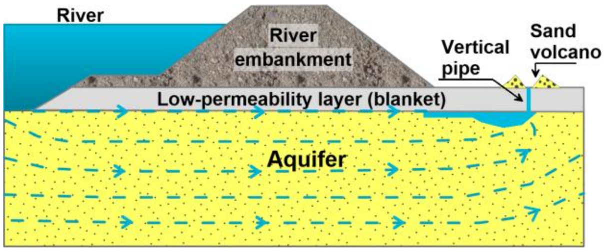

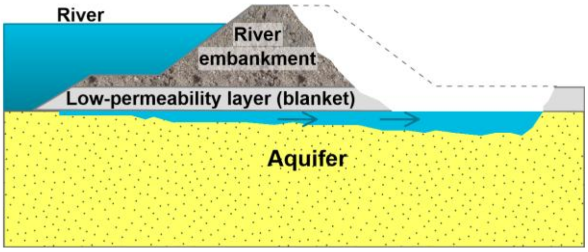

ACCEPTED MANUSCRIPT

Downloaded from http://qjegh.lyellcollection.org/ by guest on December 12, 2020

ACCEPTED MANUSCRIPT

Downloaded from http://qjegh.lyellcollection.org/ by guest on December 12, 2020

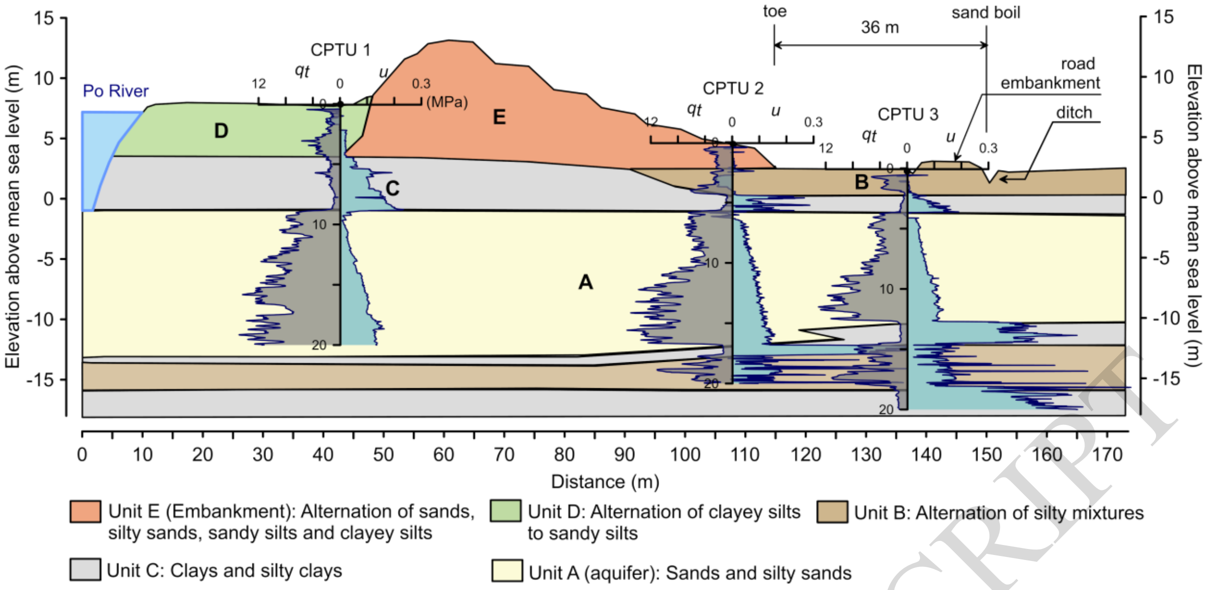

ACCEPTED MANUSCRIPT

Downloaded from http://qjegh.lyellcollection.org/ by guest on December 12, 2020

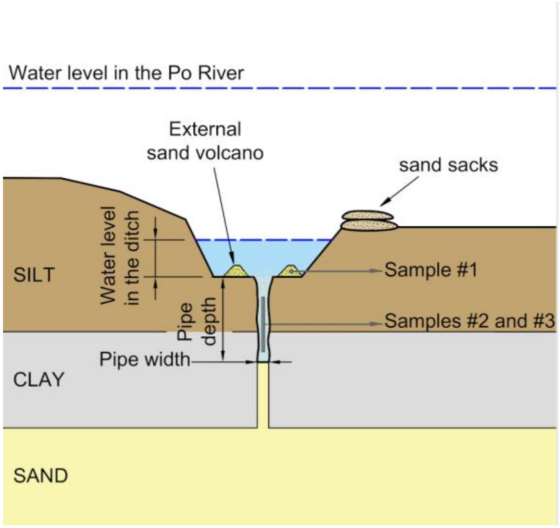

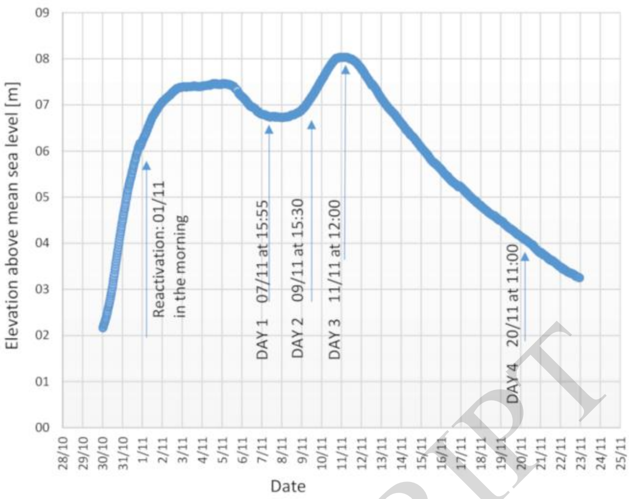

ACCEPTED MANUSCRIPT

Downloaded from http://qjegh.lyellcollection.org/ by guest on December 12, 2020

ACCEPTED MANUSCRIPT

Downloaded from http://qjegh.lyellcollection.org/ by guest on December 12, 2020

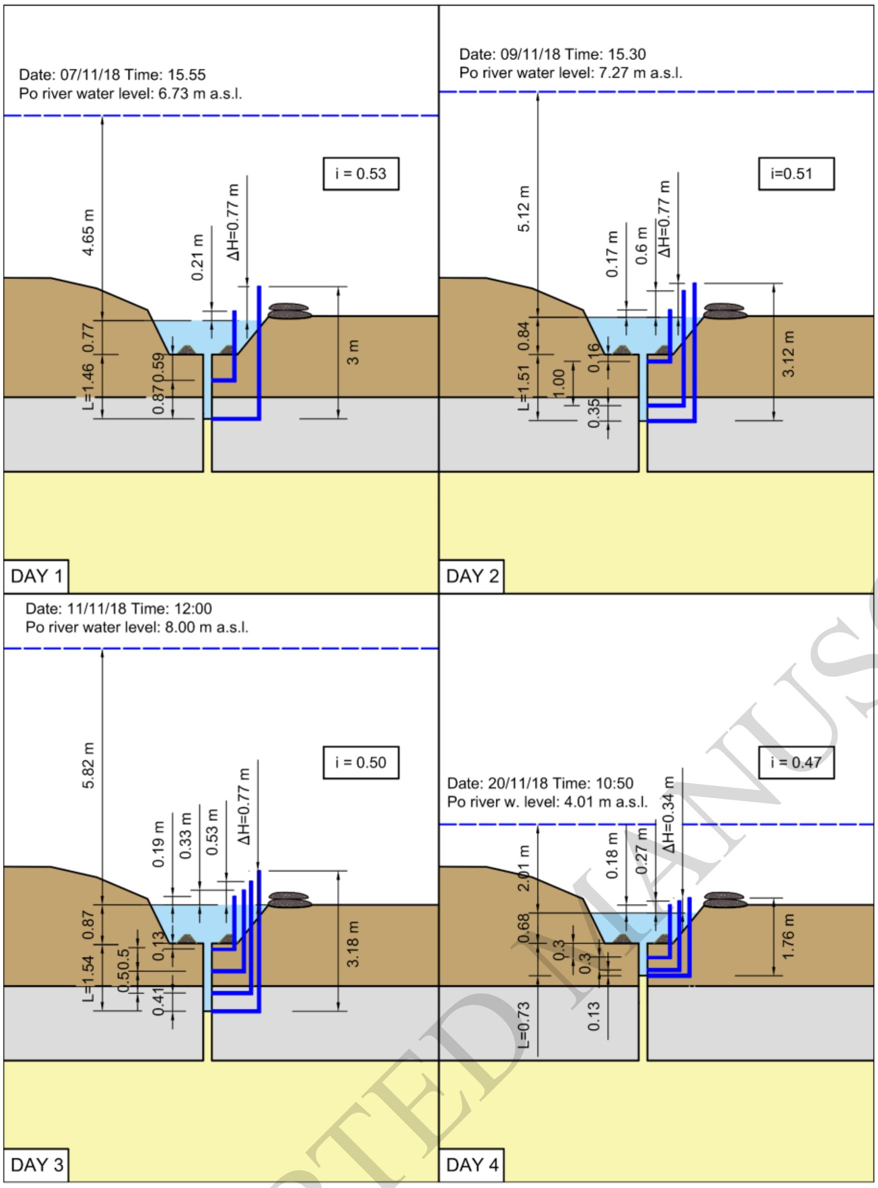

ACCEPTED MANUSCRIPT

Downloaded from http://qjegh.lyellcollection.org/ by guest on December 12, 2020

ACCEPTED MANUSCRIPT

Downloaded from http://qjegh.lyellcollection.org/ by guest on December 12, 2020

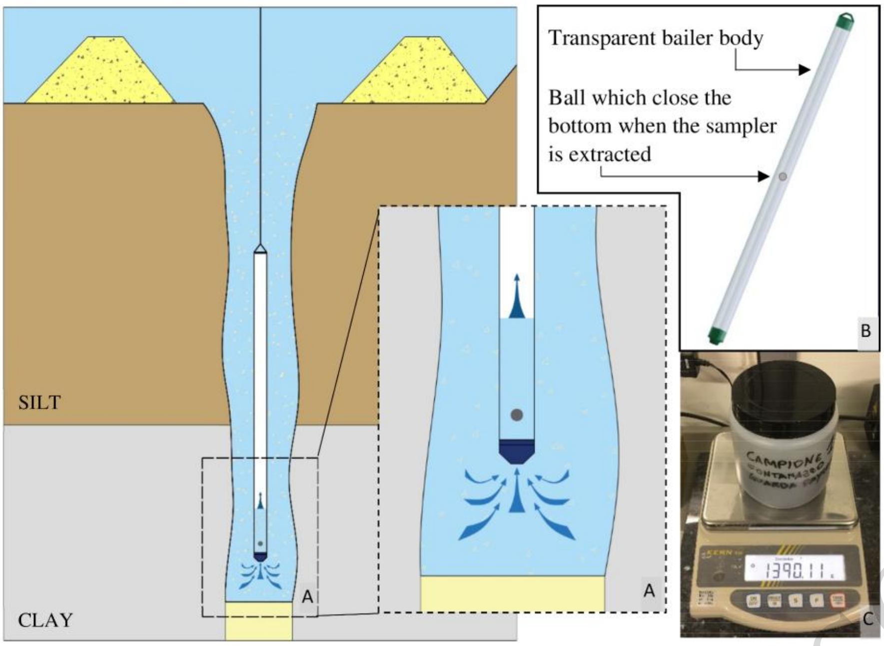

ACCEPTED MANUSCRIPT

Downloaded from http://qjegh.lyellcollection.org/ by guest on December 12, 2020

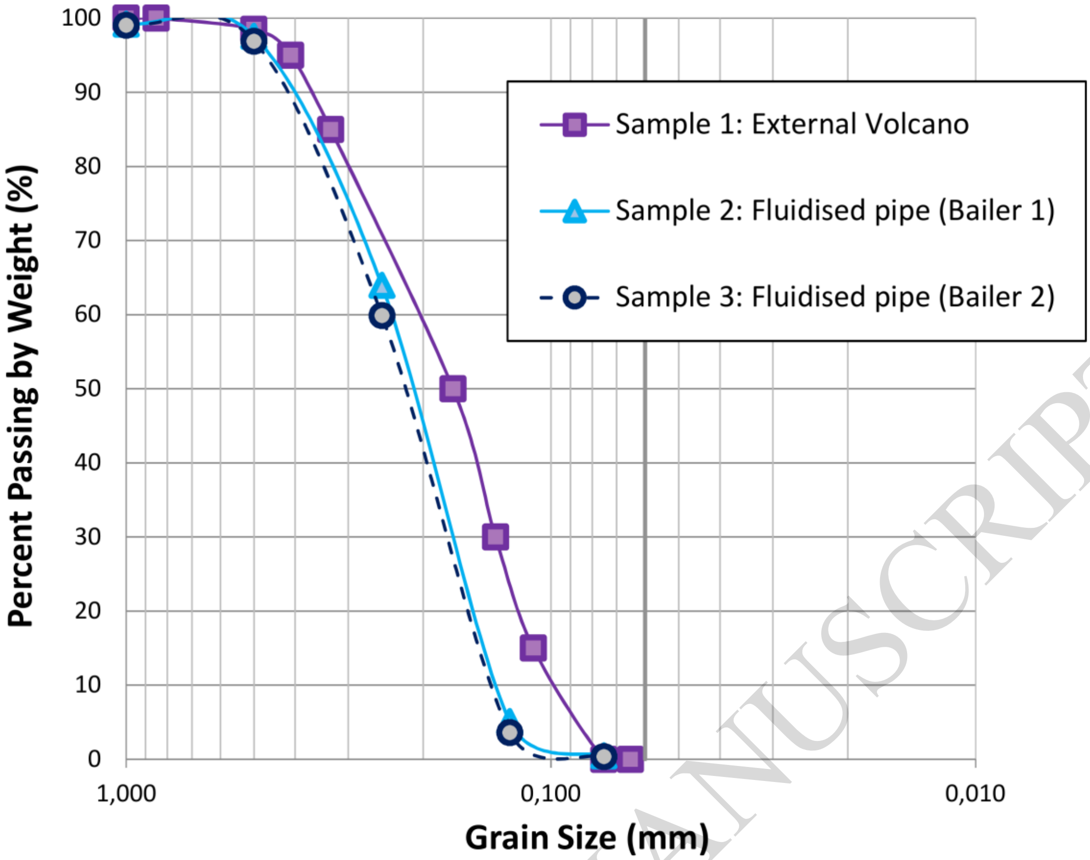

ACCEPTED MANUSCRIPT

Downloaded from http://qjegh.lyellcollection.org/ by guest on December 12, 2020

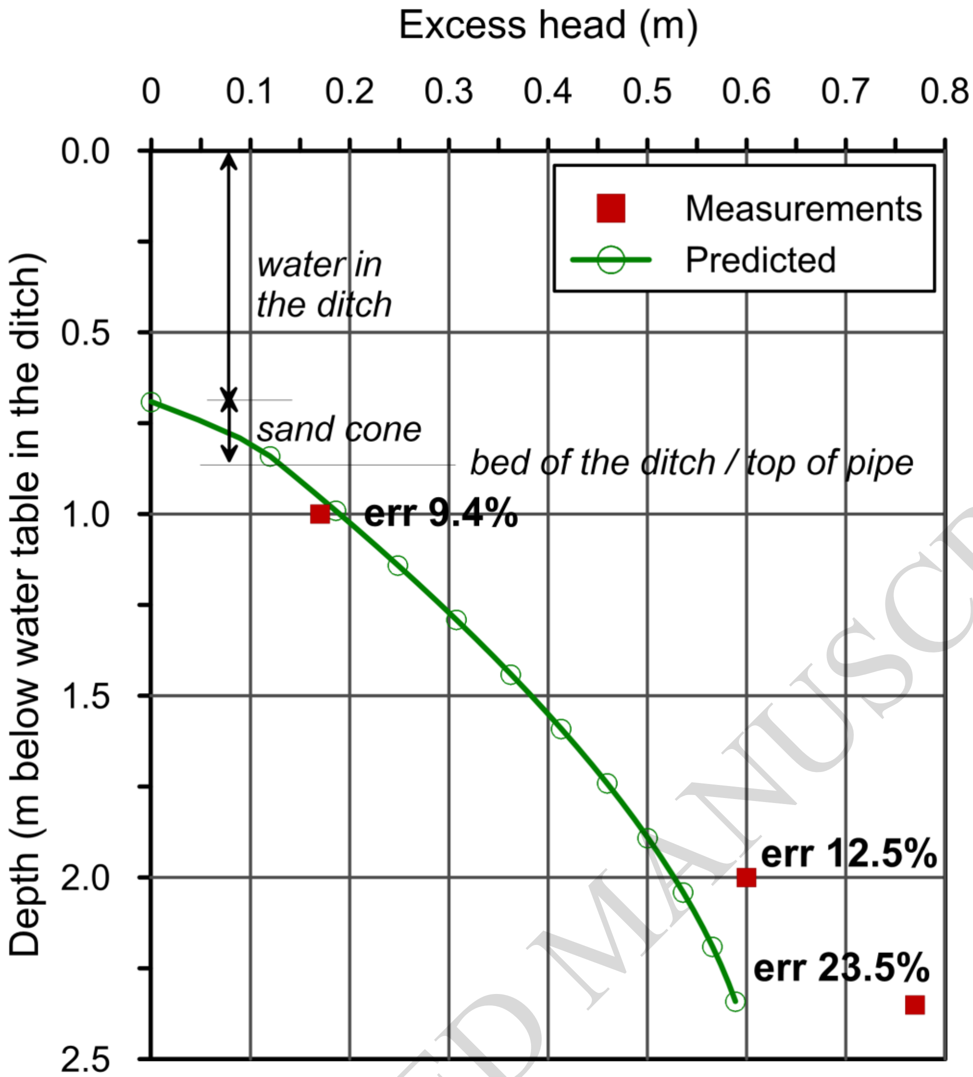

ACCEPTED MANUSCRIPT

Downloaded from http://qjegh.lyellcollection.org/ by guest on December 12, 2020

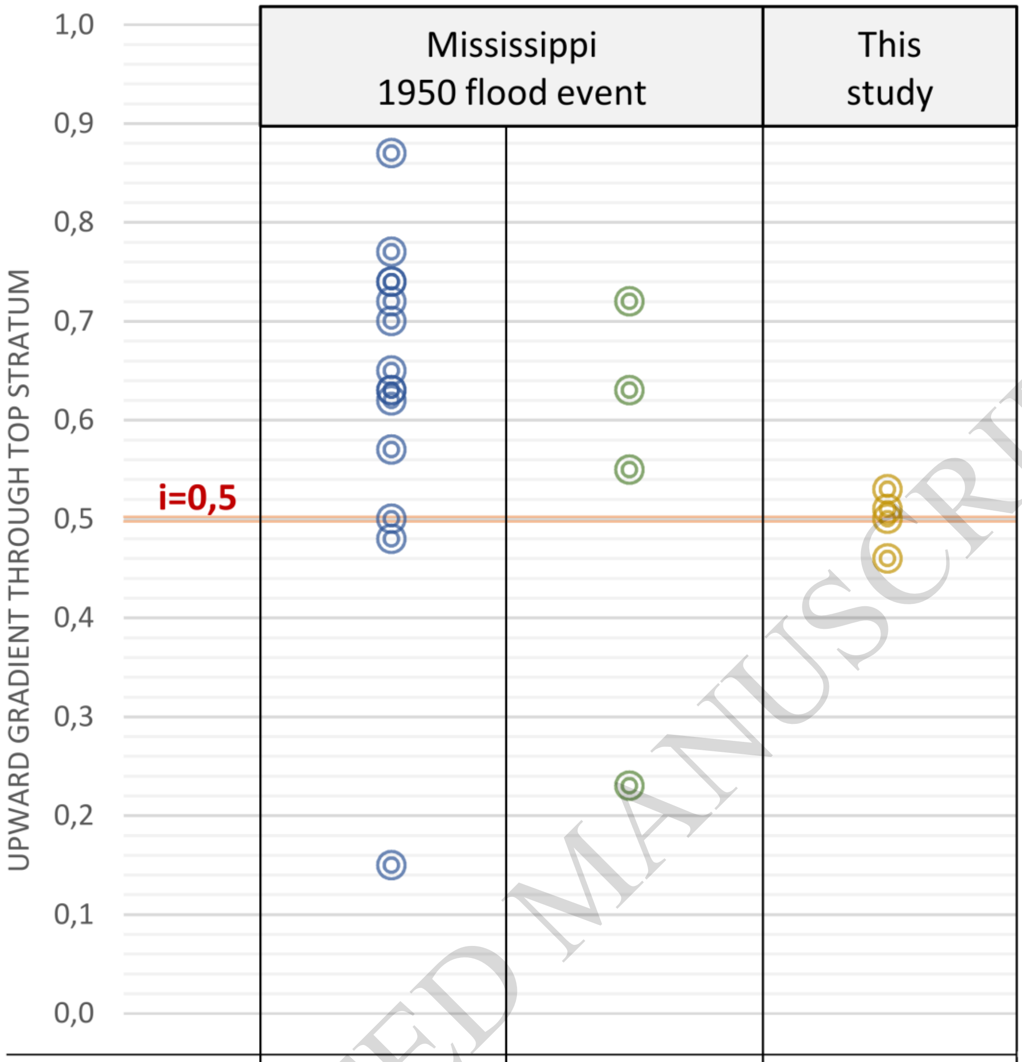

	Mississippi 1950 flood event		This study
Severity of the sand boil	numerous and/or large sand boils	numerous pin boils or several small boils	single large sand boil
Condition of the sand boil when the gradient was measured	onset of activation	onset of activation	Equilibrium phase
New activation or reactivation	Not specified	Not specified	Reactivation

ACCEPTED MANUSCRIPT

Downloaded from http://qjegh.lyellcollection.org/ by guest on December 12, 2020

Day (dd/mm/year)	z_w (m a.s.l.)	D (m)	L (m)	Q (l/s)	$\Delta H_{river\text{-}ditch}$ (m)	$h_{pipe\ base}$ (m)	ΔH (m)	$i=\Delta H/L$ (-)
07/11/2018	6.73	-	1,46	-	4.65	3,00	0,77	0,53
09/11/2018	7.27	0,20-0,35	1,51	2	5.12	3.12	0,77	0,51
11/11/2018	8.00	-	1,54	-	5.82	3.18	0,77	0,50
20/11/2018	4.01	-	0,73	-	2.01	1.76	0,34	0,46

ACCEPTED MANUSCRIPT

Downloaded from http://qjegh.lyellcollection.org/ by guest on December 12, 2020

Input parameter	
n_{min}	0.40
G_s	2.65
d_{98} (mm)	0.35
ρ_w (kg/m^3)	1000
ρ_s (kg/m^3)	2650
g (m/s^2)	9.81
μ (Pa· s)	$1 \cdot 10^{-3}$
D_{top} (m)	0.35
D_{base} (m)	0.20
α (°)	15
Q (m^3/s)	$2 \cdot 10^{-4}$

ACCEPTED MANUSCRIPT